INTERNATIONAL JOURNAL FOR NUMERICAL METHODS IN FLUIDS, VOL. 23, 415–430 (1996)

EFFICIENT ANALYTIC SERIES SOLUTIONS FOR TWO-DIMENSIONAL POTENTIAL FLOW PROBLEMS

A. W. GILL* AND W. W. READ†

Department of Mathematics and Statistics, James Cook University of North Queensland, Townsville, Qld. 4811, Australia

SUMMARY

The solution of Laplace's equation for a wide range of spatial domains and boundary conditions is a valuable asset in the study of potential theory. Recently, classical analytic series techniques based on separation of variables have been modified to solve Laplace's equation with both irregular and free boundaries. Computationally the free boundary problem is reduced to an iterative sequence of curve-fitting exercises. At each iteration the series coefficients for a known boundary problem are evaluated numerically. In this paper a new interpolation approach is presented for the estimation of the series coefficients. It has the advantages of providing a conceptually simpler view of the series technique and of estimating the series coefficients significantly faster than alternative approaches. Owing to the choice of basis functions in the truncated series solution, rigorous estimates of the error in the approximation are immediately available. A free boundary problem from steady hillside seepage with irregular boundaries will be used to illustrate the new technique.

KEY WORDS: potential flow; free boundary; analytic series; arbitrary boundaries; steady seepage

1. INTRODUCTION

The study of potential theory is based on solutions of Laplace's equation, one of the most commonly occurring equations in applied mathematics.[1] Applications frequently arise in fluid mechanics and solutions are often sought for a wide range of spatial domains and boundary conditions. Solution methods are typically numerical and include boundary integral[2] and finite element methods[3] and (less commonly) spectral methods.[4,5] Unfortunately, numerical schemes have the propensity to be computationally expensive and cumbersome to implement, with accurate error estimates not always immediately available.

Numerical procedures based on analytical techniques are preferable as they can provide computationally efficient ways of producing accurate, reliable solutions. Solutions thus obtained are inherently valuable as they can also be used to check the results of purely numerical schemes. Conformal transformations can provide closed-form analytical solutions,[6] but for a large range of boundary geometries, suitable transformations are not easily found.

Classical analytic series solutions obtained by separation of variables[7] satisfy the partial differential equation, some (but not all) of the boundary conditions exactly. This is in direct contrast with spectral methods, where the partial differential equation is not satisfied exactly and the boundary conditions usually are. This has important implications for the efficiency and accuracy of the solution technique. In particular, the dimension of the problem can be reduced by one, using analytic basis

* Current address: Applied Mathematics Department, University of Adelaide, Adelaide, S.A. 5005, Australia.
† Corresponding author.

CCC 0271–2091/96/050415–16

Received 27 April 1995
Revised 8 November 1995

functions. Additionally, rigorous estimates of the maximum error of the (analytic) truncated series solution are immediately available from the boundary errors. However, classical analytic series techniques have had limited application, as the method generally relies on regular, known boundaries. Analytical techniques encounter further difficulties in free boundary problems, where at least one boundary is initially unknown.

Recently the classical series solution has been modified to solve Laplace's equation with both irregular and free boundaries.[8,9] The free boundary location is first estimated, then iteratively improved by solving a known boundary value problem at each step, using one of the free boundary conditions as a cost function. For the solution of the known boundary value problem, the series coefficients are estimated using numerical techniques. These techniques include quasi-least squares,[9,10] least squares[8] and eigenfunction expansions.[11]

A comparison of these analytic series techniques has recently been performed for Laplacian free boundary problems,[12] from which the eigenfunction expansion method appears to be the most suitable. In particular it provides a general theoretical framework for the series solution as well as a comparatively efficient procedure for determining the series coefficients.

In this paper a new approach is presented for the efficient estimation of the analytic series coefficients, derived from interpolation or pseudospectral methods.[5,13] Although the theoretical basis for this new approach is not immediately obvious, it relies implicitly on the same underlying assumptions as the eigenfunction expansion method. Moreover, the new method provides a conceptually simpler view of the series technique and, more importantly, a significantly faster procedure for estimating the series coefficients.

This paper is organized into six sections. Following this introduction, the Laplacian free boundary problem is formulated in Section 2. The general analytic series solution is presented in Section 3, before detailing two techniques, eigenfunction expansion and interpolation, for estimating the series coefficients in Section 4. The interpolation method will be illustrated in Section 5, where a free boundary problem from steady hillside seepage is solved. Finally, a discussion of the results is presented in Section 6.

2. POTENTIAL FLOW PROBLEMS

Laplace's equation in the plane,

$$\frac{\partial^2 \phi}{\partial x^2} + \frac{\partial^2 \phi}{\partial y^2} = 0, \tag{1}$$

governs the solution $\phi(x, y)$ on the interior of the domain in Figure 1 (ABDEFGHA) to which suitable boundary conditions are applied. Assuming vertical and impermeable side boundaries at $x = 0$ (AH) and $x = s$ (CE), one then has

$$\left.\frac{\partial \phi}{\partial x}\right|_{x=0} = 0, \qquad \left.\frac{\partial \phi}{\partial x}\right|_{x=s} = 0. \tag{2}$$

The bottom boundary (HGFE), defined by $y = f^b(x)$, is arbitrary but also assumed impermeable. The normal derivative along this curve is required to be zero, so that

$$\dot{f}^b(x) \left.\frac{\partial \phi}{\partial x}\right|_{y=f^b(x)} - \left.\frac{\partial \phi}{\partial y}\right|_{y=f^b(x)} = 0, \tag{3}$$

where the dot denotes differentiation with respect to x.

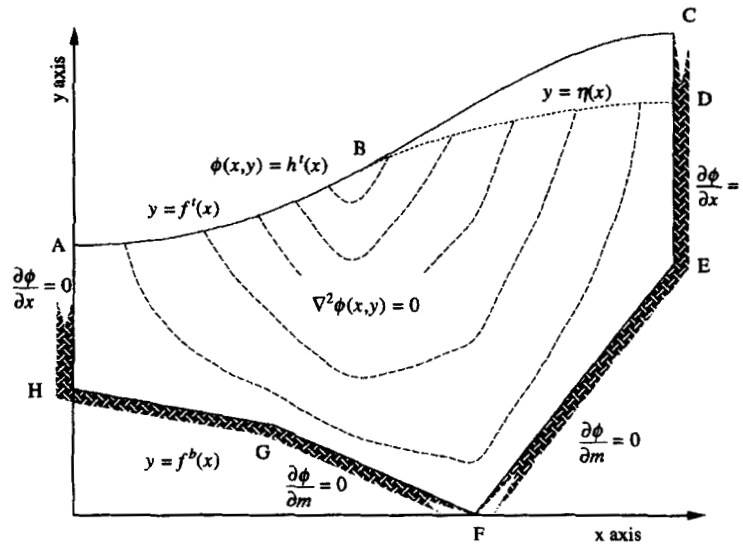

Figure 1. The boundary value problem to be solved. Laplace's equation governs the interior, supplemented by various conditions on the boundaries

The top boundary, defined by

$$y = y^t(x) = \begin{cases} f^t(x), & 0 \leqslant x < r, \\ \eta(x), & r \leqslant x \leqslant s, \end{cases} \tag{4}$$

consists of an arbitrary (but known) segment $f^t(x)$ (AB) and an unknown segment $\eta(x)$ (BD) which is referred to as a free boundary. The length of the free boundary, determined by r, is also unknown. Along the entire top boundary (ABD) the solution is subject to a Dirichlet boundary condition

$$\phi[x, y^t(x)] = h^t(x), \tag{5}$$

whilst along the free boundary component (BD) the Neumann boundary condition

$$\dot{\eta}(x)\frac{\partial \phi}{\partial x}\bigg|_{y=\eta(x)} - \frac{\partial \phi}{\partial y}\bigg|_{y=\eta(x)} = -\dot{h}^t(x)\sqrt{\{1 + [\dot{\eta}(x)]^2\}} \tag{6}$$

is also imposed. Unfortunately, this boundary condition is non-linear and implicit in $\eta(x)$. However, (6) can be linearized[8] by introducing a conjugate streamfunction $\psi(x, y)$ which is related to $\phi(x, y)$ by the Cauchy–Riemann equations

$$\frac{\partial \phi}{\partial x} = \frac{\partial \psi}{\partial y}, \qquad \frac{\partial \phi}{\partial y} = -\frac{\partial \psi}{\partial x}. \tag{7}$$

Substituting into (6) yields

$$\frac{\partial \psi}{\partial x}\bigg|_{y=\eta(x)} + \frac{\partial \psi}{\partial y}\frac{dy}{dx}\bigg|_{y=\eta(x)} = \frac{d\psi}{dx}\bigg|_{y=\eta(x)} \tag{8}$$

$$= -\dot{h}^t(x)\sqrt{\{1 + [\dot{\eta}(x)]^2\}}. \tag{9}$$

Integrating the right-hand sides with respect to x, the Neumann condition becomes

$$\psi(x, \eta) = -\int \dot{h}^{t}(x)\sqrt{\{1 + [\dot{\eta}(x)]^2\}}\, dx. \tag{10}$$

The solution $\phi(x, y)$ and free boundary $\eta(x)$ are then determined by solving Laplace's equation (1) subject to the boundary conditions (2), (3), (5) and (10). This can be achieved by assuming an initial location for the free boundary and solving the corresponding known boundary value problem. The estimated free boundary is then updated using the streamfunction condition (10) as a cost function. This procedure is continued until a predefined error tolerance is satisfied.

2.1. The free boundary

The unknown boundary $\eta(x)$ can be approximated by cubic splines[14] as

$$\eta(x) = \sum_{i=1}^{4} d_{ij} \frac{(x - \xi_j)^{i-1}}{(i-1)!}, \quad x \in \tau_j, \tag{11}$$

within $L - 1$ subintervals $\tau_j = [\xi_j, \xi_{j+1}], j = 1, 2, \ldots, L - 1$, defined by breakpoints satisfying

$$r = \xi_1 < \xi_2 < \cdots < \xi_{L-1} < \xi_L = s. \tag{12}$$

Cubic splines are widely available in numerical software packages and provide smooth continuous interpolants once the spline coefficients d_{ij} are determined. The known boundaries $f^{t}(x)$ and $f^{b}(x)$ can be used to construct an initial estimate by setting $r = s/2, \eta_1 = f^{t}(r)$ and $\eta_L = [f^{t}(s) + f^{b}(s)]/2$. The remaining free boundary locations $\eta_j, j = 2, \ldots, L - 1$, are determined by fitting a single spline segment between (ξ_1, η_1) and (ξ_L, η_L).

Once the known boundary value problem (1)–(3), (5) is solved, the solution can be used to update the free boundary locations using the streamfunction condition (10) as a cost function. Denoting estimates at the ith iteration by a superscript (i), the updated estimates are given by

$$\eta_j^{(i+1)} = \eta_j^{(i)} - \Delta\eta_j^{(i)}, \tag{13}$$

where the free boundary increments $\Delta\eta_j^{(i)}$ are given by

$$\Delta\eta_j^{(i)} = c^{(i)}(\psi(x, \eta) + \int \dot{h}^{t}(x)\sqrt{\{1 + [\dot{\eta}(x)]^2\}}\, dx), \tag{14}$$

with $c^{(i)}$ chosen (usually as a constant) to enhance the convergence rate of the scheme (see e.g. Reference 14).

3. THE ANALYTIC SERIES SOLUTION

The method of separation of variables[7,15] can be used to obtain an analytic series solution to Laplace's equation (1) subject to the side boundary conditions (2). Assuming that $\phi(x, y) = F(x)G(y)$, Laplace's equation can be separated into two second-order ordinary differential equations

$$\ddot{F}(x) + \lambda F(x) = 0 \tag{15}$$

and

$$\ddot{G}(y) - \lambda G(y) = 0, \tag{16}$$

where λ is the constant of separation. The impermeable, vertical side boundary conditions (2) imply $\dot{F}(0) = 0$ and $\dot{F}(s) = 0$, so that the solutions to (15) are

$$F_n(x) = \cos(n\pi x/s) \quad \text{and} \quad \lambda_n = (n\pi/s)^2, \quad n = 0, 1, 2, \ldots. \tag{17}$$

With the constant of separation specified, the general solution to (16) is then

$$G_n(y) = \begin{cases} \alpha_0 + \beta_0 y, & n = 0, \\ \alpha_n \cosh(n\pi y/s) + \beta_n \sinh(n\pi y/s), & n \geqslant 1, \end{cases} \tag{18}$$

where the α_n and β_n are constants. The general solution to Laplace's equation (1) subject to the boundary conditions (2) is then given by

$$\phi(x, y) = \alpha_0 + \beta_0 y + \sum_{n=1}^{\infty} [\alpha_n u_n(x, y) + \beta_n v_n(x, y)], \tag{19}$$

where

$$u_n(x, y) = \cosh(n\pi y/s)\cos(n\pi x/s), \tag{20}$$

$$v_n(x, y) = \sinh(n\pi y/s)\cos(n\pi x/s). \tag{21}$$

The bottom and top boundary conditions (3) and (5) are then used to determine the series coefficients α_n and $\beta_n (n = 0, 1, 2, \ldots)$. Substituting (19) into (3) and (5) yields the equations

$$\sum_{n=0}^{\infty} [\alpha_n \bar{u}_n^{\mathrm{b}}(x) + \beta_n \bar{v}_n^{\mathrm{b}}(x)] = 0, \tag{22}$$

$$\sum_{n=0}^{\infty} [\alpha_n u_n^{\mathrm{t}}(x) + \beta_n v_n^{\mathrm{t}}(x)] = h^{\mathrm{t}}(x), \tag{23}$$

where $\bar{u}_0^{\mathrm{b}}(x) = 0$, $u_0^{\mathrm{t}}(x) = 1$, $\bar{v}_0^{\mathrm{b}}(x) = -s/\pi$, $v_0^{\mathrm{t}}(x) = y^{\mathrm{t}}(x)$ and for $n \geqslant 1$

$$\bar{u}_n^{\mathrm{b}}(x) = n\dot{f}^{\mathrm{b}}(x)\cosh[n\pi f^{\mathrm{b}}(x)/s]\sin(n\pi x/s) + n\sinh[n\pi f^{\mathrm{b}}(x)/s]\cos(n\pi x/s), \tag{24}$$

$$\bar{v}_n^{\mathrm{b}}(x) = n\dot{f}^{\mathrm{b}}(x)\sinh[n\pi f^{\mathrm{b}}(x)/s]\sin(n\pi x/s) + n\cosh[n\pi f^{\mathrm{b}}(x)/s]\cos(n\pi x/s), \tag{25}$$

$$u_n^{\mathrm{t}}(x) = \cosh[n\pi y^{\mathrm{t}}(x)/s]\cos(n\pi x/s), \tag{26}$$

$$v_n^{\mathrm{t}}(x) = \sinh[n\pi y^{\mathrm{t}}(x)/s]\cos(n\pi x/s). \tag{27}$$

If the bottom boundary is horizontal, $f^{\mathrm{b}}(x) = f^{\mathrm{b}}$, then (22) admits the simple relationships

$$\beta_0 = 0 \quad \text{and} \quad \beta_n = -\alpha_n \tanh(n\pi f^{\mathrm{b}}/s), \quad n \geqslant 1, \tag{28}$$

between the series coefficients. These results occur since the functions $\bar{u}_n^{\mathrm{b}}(x)$ and $\bar{v}_n^{\mathrm{b}}(x)$ are both proportional to the Fourier cosines $\cos(n\pi x/s)$ in that case. The linear independence of these functions then guarantees (28). Similarly, if the top boundary is constant, $y^{\mathrm{t}}(x) = f^{\mathrm{t}}$, then (23) and (28) imply

$$\sum_{n=0}^{\infty} \hat{\alpha}_n \cos(n\pi x/s) = h^{\mathrm{t}}(x), \tag{29}$$

where the $\hat{\alpha}_n = \alpha_n[\cosh(n\pi f^{\mathrm{t}}/s) - \tanh(n\pi f^{\mathrm{b}}/s)\sinh(n\pi f^{\mathrm{t}}/s)]$ are easily identified as the Fourier cosine coefficients of the function $h^{\mathrm{t}}(x)$. The orthogonality of the Fourier cosines then permits computationally efficient evaluation of these coefficients.

However, if either the top or bottom boundary is not constant, the 'classical' approach above breaks down. The functions (24) and (25) or (26) and (27) are now no longer proportional, which leaves the relationships (22) and (23) between the series coefficients functionally dependent on x. Mathematically the boundaries are not co-ordinate curves whereby one variable remains constant. A change of co-ordinates may be found to achieve this; however, the new system may not allow a solution by separation of variables. For Laplace's equation there are 11 three-dimensional co-ordinate systems which enable direct separation,[16] but, for example, for a simple parallelogram there is no such system.

Until recently this has discouraged researchers from persisting with the analytic series solution. However, alterative or 'non-classical' methods can be developed to estimate the series coefficients in (22) and (23). The first to do so were Powers *et al.*,[17] who considered a linear top boundary and a horizontal base at finite depth. Their method was to expand the functions (26) and (27) in terms of orthonormal functions using the Gram–Schmidt process. Extensions to an arbitrary top boundary[18] and a horizontal base at infinite depth[19] soon followed.

The series method was first extended to cater for sloping-based problems by Read and Volker,[20] whereby both sets of coefficients need to be estimated. Quasi-least squares,[10] least squares[8] and eigenfunction expansions[11] have all been investigated as possible estimation techniques. The third technique has also provided a strong theoretical framework for the general analytic series solution and is described in the next section. With the theoretical basis established, a new approach is then presented which has the advantages of being both conceptually simpler and computationally more efficient.

4. ESTIMATING THE SERIES COEFFICIENTS

In practice not all the series coefficients in (19) can be evaluated or in general calculated exactly. Consequently the approximation

$$\phi_N(x, y) = a_0 + b_0 y + \sum_{n=1}^{N-1} [a_n u_n(x, y) + b_n v_n(x, y)] \tag{30}$$

is used instead, where a_n and b_n, $n = 0, 1, 2, \ldots, N-1$, are generally only approximations to the corresponding analytic series coefficients. Note, however, that $\phi_N(x, y)$ satisfies both Laplace's equation (1) and the side boundary conditions (2) exactly. Any error incurred will be from the violation, if any, of the bottom or top boundary conditions (3) or (5) by $\phi_N(x, y)$. This may be written as

$$\sum_{n=0}^{N-1} [a_n \bar{u}_n^{\mathrm{b}}(x) + b_n \bar{v}_n^{\mathrm{b}}(x)] = R_N^{\mathrm{b}}(x; \mathbf{a}, \mathbf{b}), \tag{31}$$

$$\sum_{n=0}^{N-1} [a_n u_n^{\mathrm{t}}(x) + b_n v_n^{\mathrm{t}}(x)] - h^{\mathrm{t}}(x) = R_n^{\mathrm{t}}(x; \mathbf{a}, \mathbf{b}), \tag{32}$$

where $R_N^{\mathrm{b}}(x; \mathbf{a}, \mathbf{b})$ and $R_n^{\mathrm{t}}(x; \mathbf{a}, \mathbf{b})$ are the residual errors in $\phi_N(x, y)$ on the bottom and top boundaries respectively and $\mathbf{a}$ and $\mathbf{b}$ represent the series coefficients a_i and b_i, $k = 0, 1, 2 \ldots, N-1$, respectively.

A powerful property of the analytic series (30) (see Section 5) is that the maximum (and minimum) values of the error in the solution will occur on either the top or bottom boundaries, so that attention may be focused on the solutions to (31) and (32), which are equations in only one spatial variable. The best practical solution would be one that minimizes both residual errors $R_N^{\mathrm{b}}(x; \mathbf{a}, \mathbf{b})$ and $R_N^{\mathrm{t}}(x; \mathbf{a}, \mathbf{b})$ in some sense, so that the analytic series technique is essentially a one-dimensional curve-fitting exercise, but where double expansions are used. The eigenfunction expansion method[10,11] has provided a theoretical basis for these expansions and an outline of that method is presented in the next subsection. A new approach which is far more efficient is then presented.

4.1. Eigenfunction expansions

The difficulty in computing the series coefficients for non-constant bottom and top boundaries arises from the functions $\bar{u}_n^b(x)$ being dissimilar to the functions $\bar{v}_m^b(x)$ (and likewise for $u_n^b(x)$ and $v_n^b(x)$). Assuming that the $\bar{v}_n^b(x)$ are linearly independent and complete, in theory each $\bar{u}_n^b(x)$ can be represented as a linear combination of these functions. In practice a finite sum is used and an approximation is constructed:

$$\bar{u}_n^b(x) \approx \sum_{i=0}^{N-1} F_{in}^{ub} \bar{v}_i^b(x), \quad n = 0, 1, 2, \ldots, N-1, \tag{33}$$

where the F_{in}^{ub} are expansion coefficients.

Substituting this expansion into the left-hand side of (31) and setting this equal to zero, some rearrangement yields the equation

$$\sum_{n=0}^{N-1} \left(\sum_{i=0}^{N-1} F_{ni}^{ub} a_i + b_n \right) \bar{v}_n^b(x) = 0. \tag{34}$$

The linear independence of the $\bar{v}_n^b(x)$ then produces the following relationship between the series coefficients:

$$\mathbf{b} = -F^{ub}\mathbf{a}. \tag{35}$$

Here the nth series coefficient b_n is seen to depend on possibly every coefficient a_i for $i = 0, 1, 2, \ldots, N-1$. This is to be expected, considering the connection between the functions $\bar{u}_n^b$ and $\bar{v}_n^b(x)$ defined by (33). Notice also that (35) reproduces the result (28) in the case of a horizontal bottom boundary, for which F^{ub} is diagonal.

The series coefficients a_n are estimated using the same approach for the top boundary condition (32). Approximating $u_n^t(x)$ and $h^t(x)$ by finite linear combinations of the functions $v_n^t(x)$ (again assumed linearly independent and complete) yields

$$u_n^t(x) \approx \sum_{i=0}^{N-1} F_{in}^{ut} v_i^t(x), \quad n = 0, 1, 2, \ldots, N-1, \tag{36}$$

$$h^t(x) \approx \sum_{i=0}^{N-1} h_i^t v_i^t(x). \tag{37}$$

Substituting these and the result (35) into the left-hand side of (32) and equating the resultant expression to zero produces a linear system of equations for the series coefficients a_n:

$$(F^{ut} - F^{ub})\mathbf{a} = \mathbf{h}^t. \tag{38}$$

Thus the approximate solution $\phi_N(x, y)$ is fully determined once the expansion coefficient matrices F^{ut} and F^{ub} and vector $\mathbf{h}^t$ are calculated and the linear systems (38) and (35) subsequently solved for the series coefficients $\mathbf{a}$ and $\mathbf{b}$. The expansion coefficients are determined by a least squares procedure[8] which minimizes the integral of the square of the residual errors in the approximations (33), (36) and (37). This results in systems of linear equations of the form

$$\bar{V}^b F^{ub} = G^{ub}, \qquad V^t F^{ut} = G^{ut}, \tag{39}$$

$$V^t \mathbf{h}^t = \mathbf{g}^t, \tag{40}$$

where, for $i, j = 0, 1, 2, \ldots, N-1$,

$$\bar{V}^b_{ij} = \langle \bar{v}^b_i(x), \bar{v}^b_j(x) \rangle, \qquad G^{ub}_{ij} = \langle \bar{u}^b_i(x), \bar{v}^b_j(x) \rangle, \tag{41}$$

$$V^t_{ij} = \langle v^t_i(x), v^t_j(x) \rangle, \qquad G^{ut}_{ij} = \langle u^t_i(x), v^t_j(x) \rangle, \tag{42}$$

$$g^t_j = \langle h^t(x), v^t_j(x) \rangle, \tag{43}$$

with

$$\langle f(x), g(x) \rangle = \int_0^s f(x) g(x)\, dx. \tag{44}$$

The integrations and matrix inversions are then carried out by computer using standard IMSL Fortran routines.

4.2. *The Interpolation Approach*

In free boundary problems, the efficiency of the analytic series solution is governed by the determination of the series coefficients in (30) at each iteration. The eigenfunction expansion method determines the series coefficients as solutions to linear systems whose construction requires the numerical evaluation of the inner products (41)–(43).

As an indication of the effort required (and potential difficulty) in performing such integrations, consider an element of the matrix V^t:

$$V^t_{ij} = \int_0^s \sinh[i\pi y^t(x)/s] \sinh[j\pi y^t(x)/s] \cos(i\pi x/s) \cos(j\pi x/s)\, dx. \tag{45}$$

The sinh terms produce an envelope to the cosine product and the number of quadrature points needed to resolve its oscillation must be greater than $i+j$. For the matrix elements with $i, j \sim N$ (i.e. bottom right-hand corner elements) this implies that the integration will require at least $O(N)$ time to compute. A potential numerical obstacle in evaluting these integrals is the effect of the envelope $\sinh[i\pi y^t(x)/s] \sinh[j\pi y^t(x)/s]$. As i and j get larger, the exponential character of this function is more prominent—even with a slowly varying top boundary $y^t(x)$. The numerical evaluation of integrals involving such rapidly varying and oscillating integrands can be difficult to perform.

An alternative approach which eliminates these features from the analytic series solution is derived from interpolation or pseudospectral methods. An excellent review is provided by Boyd[5] and the method is conceptually very simple to understand. It eliminates the need for further expansions such as (33), (36) and (37) and applies directly to the residual errors in $\phi_N(x, y)$.

Viewing equations (30)–(32) as an interpolation problem, the approximation $\phi_N(x, y)$ is simply forced to satisfy the bottom and top boundary conditions exactly at a set of N discrete nodes $x_i \in (0, s)$, $i = 0, 1, 2, \ldots, N-1$. Thus the series coefficients $\mathbf{a}$ and $\mathbf{b}$ are chosen so that the residual errors defined by (31) and (32) are zero at these nodes, i.e.

$$R^b_n(x_i; \mathbf{a}, \mathbf{b}) = 0 \quad \text{and} \quad R^t_N(x_i; \mathbf{a}, \mathbf{b}) = 0, \quad i = 0, 1, 2, \ldots, N-1. \tag{46}$$

The convergence of the series solution obtained using the eigenfunction expansion method depends on the completeness of the basis functions in the top and bottom boundary approximations. This assumption is explicitly stated for the convergence of the approximations of $\bar{u}^b_n(x)$, $u^t_n(x)$ and $h^t(x)$ in (33), (36) and (37) as $N \to \infty$. Alternatively, the assumption of completeness is implicit in the interpolation approach and cannot be directly related to a particular set of basis functions in the boundary approximations. However, the convergence of the series using the eigenfunction expansions

implies that the series will also converge using the interpolation method. That is, as the density of nodes increases with N, the approximate solution $\phi_N(x, y)$ converges to the analytic solution, barring round-off error.

This method also belongs to the more general method of weighted residuals of which Finlayson[21] provides a detailed account. It differs here in that the residuals are formed not from the differential equation but from the boundary conditions, since the differential equation is automatically satisfied by the series solution. As such it should be viewed as an interpolation method, since only simple function evaluations will be involved. The choice of nodes is arbitrary, but evenly spaced nodes appear to be the best. This is not surprising, since the approximation (30) is similar to a Fourier cosine expansion (see (20) and (21)). Consequently this distribution of nodes will be adopted here.

The conditions (46) result in $2N$ linear equations for the $2N$ series coefficients $\mathbf{a}$ and $\mathbf{b}$, which may be written as

$$F^{ub}\mathbf{a} + F^{vb}\mathbf{b} = \mathbf{0}, \qquad F^{ut}\mathbf{a} + F^{vt}\mathbf{b} = \mathbf{h}^t, \tag{47}$$

where for $i, j = 0, 1, 2, \ldots, N-1$

$$F_{ij}^{ut} = u_j^t(x_i), \qquad F_{ij}^{vt} = v_j^t(x_i), \tag{48}$$

$$F_{ij}^{ub} = \bar{u}_j^b(x_i), \qquad F_{ij}^{vb} = \bar{v}_j^b(x_i), \tag{49}$$

$$h_i^t = h^t(x_i). \tag{50}$$

These equations may be rearranged to give

$$\mathbf{b} = -(F^{vb})^{-1}F^{ub}\mathbf{a}, \tag{51}$$

$$[F^{ut} - F^{vt}(F^{vv})^{-1}F^{ub}]\mathbf{a} = \mathbf{h}^t, \tag{52}$$

which resemble equations (35) and (38) for the eigenfunction expansion method, except for the appearance of the additional matrices F^{vt} and F^{vb}.

As mentioned above, the distinct advantage of the interpolation approach in terms of computational efficiency is that no inner products need to be evaluated. To illustrate this advantage Table I compares typical execution times for the eigenfunction expansion and interpolation methods for determining the series coefficents for various values of N. From this one can clearly see the significant potential in adopting the interpolation approach. The eigenfunction expansion method is considerably slower, with the majority of the execution time spent on evaluating the inner products in (41)–(43). The interpolation method avoids this, as only simple function evaluations are required to construct the appropriate matrices.

Table I. Comparison of typical execution times (in seconds) of eigenfunction expansion (EE) and interpolation (INT) methods to determine series coefficients for various values of N

N	EE	INT
10	1·2	0·07
20	11·8	0·10
30	52·5	0·16
40	149·3	0·27
50	336·8	0·49

5. NUMERICAL RESULTS

In this section the interpolation method is demonstrated on a free boundary problem typical of steady hillside seepage problems. Steady seepage through a homogeneous aquifer is governed by Darcy's law, which reduces to Laplace's equation in the saturated flow domain when the hydraulic conductivity K is constant. For these problems, ϕ is the hydraulic potential, with the Darcian velocities given by $(-K\partial\phi/\partial x, -K\partial\phi/\partial y)$. The Neumann boundary conditions (2) and (3) correspond to an aquifer lying on top of an impermeable aquiclude, with the lateral extremities of the flow domain delineated by vertical, impermeable dykes.

A steady water table will form under the soil surface when the aquifer is subject to a (constant) vertical recharge KR below the threshold necessary for complete saturation. The upper (saturated) flow boundary consists of the seepage face $f^t(x)$, $0 \leqslant x \leqslant r$, and the water table $\eta(x)$, $r < x < s$. Along this boundary the potential is equal to the elevation above an arbitrary datum and $h^t(x) = y^t(x)$ in (5):

$$\phi[x, y^t(x)] = y^t(x). \tag{53}$$

Flow across the free boundary must be conserved and (noting that the recharge is vertical) $\dot{H}^t(x) = R/\sqrt{\{1 + [\dot{\eta}(x)]^2\}}$ in (10):

$$\psi(x, \eta) = -\int R\,dx = -Rx + \text{constant}. \tag{54}$$

Choosing the streamfunction as zero on the impermeable dykes and the aquiclude, the streamfunction condition becomes

$$\psi(x, \eta) = R(s - x). \tag{55}$$

Assuming continuity of the seepage velocities, the slope $\dot{\eta}(r)$ at the intersection of the water table and the seepage face will be given by

$$\dot{\eta}(r) = \dot{f}^t(r). \tag{56}$$

At the upstream extremity of the aquifer the water table will intersect a vertical, impermeable dyke. At this point the recharge across the water table will be vertical and the slope of the water table will be zero:

$$\dot{\eta}(s) = 0. \tag{57}$$

The streamfunction condition needs some further modification before it can be used as a cost function in the solution process. At the upstream extremity of the water table ($x = s$) the streamfunction will automatically satisfy (55) independently of the value of $\eta(s)$. This difficulty can be overcome by replacing the streamfunction estimates ψ_j at the breakpoints (ξ_j, η_j) by an averaged value $\hat{\psi}_j$:

$$\begin{aligned}\hat{\psi}_j &= \int_{\xi_j - \Delta\xi_j^-}^{\xi_j + \Delta\xi_j^+} \psi[x, \eta(x)]\,dx \\ &= \int_{\xi_j - \Delta\xi_j^-}^{\xi_j + \Delta\xi_j^+} R(s - x)\,dx \\ &= \frac{R(\Delta\xi_j^+ + \Delta\xi_j^-)[2(s - \xi_j) - (\Delta\xi_j^+ - \Delta\xi_j^-)]}{2},\end{aligned} \tag{58}$$

where $\Delta\xi_j^-$ and $\Delta\xi_j^+$ are appropriate increments on either side of the breakpoints.

The recharge at the breakpoints can then be estimated by

$$\hat{R}_j = \frac{2\hat{\psi}_j}{(\Delta\xi_j^+ + \Delta\xi_j^-)[2(s-\xi_j) - (\Delta\xi_j^+ - \Delta\xi_j^-)]} \tag{59}$$

and the water table updates $\Delta\eta_j^{(i)}$ in (13) at iteration (i) become

$$\Delta\eta_j^{(i)} = c^{(i)}(\hat{R}_j - R). \tag{60}$$

For evenly spaced breakpoints, $\Delta\xi_j^- = \Delta\xi_j^+ = (s-r)/(L-1)$ at the internal breakpoints. At the intersection of the free surface and the water table (i.e. $x = \xi_1 = r$), $\Delta\xi_1^- = 0$, while at the last breakpoint (i.e. $x = \xi_L = s$), $\Delta\xi_L^+ = 0$. At each iteration, r must be estimated before the updates for the water table at the internal breakpoints can be calculated. Noting that $\eta(x) = f^t(x)$ at the intersection of the soil surface and the water table, r can be obtained from $\eta_1^{(i+1)}$ by solving the implicit equation

$$f^t(r) = \eta_1^{(i+1)}. \tag{61}$$

5.1. *Flow solutions*

Two aquifer geometries have been chosen to demonstrate the interpolation method. In the first instance, a 'canonical' hillslope geometry has been chose, while the second example is of more general shape. The soil surface and basal geometries of aquifer 1 consist of parallel, linear segments at a slope of 5% to the horizontal. The soil surface of aquifer 2 is specified by cubic spline interpolants, while the basal geometry consists of piecewise continuous linear segments. The breakpoints, etc. for both aquifers are given in Table II.

The recharge rate for each aquifer must be chosen and an initial estimate of the water table location determined. The recharge rate used for aquifer 1 was $R = 1{\cdot}5 \times 10^{-3}$, while the rate for aquifer 2 was $R = 10^{-4}$. Initially the water table was approximated using one spline segment with $r = s/2$, $\eta_1^{(0)} = f^t(r)$ and $\eta_L^{(0)} = [f^t(s) + f^b(s)]/2$. The endpoint derivative conditions necessary to fully define the spline approximation are given by (56) and (57).

The series coefficients for $\phi_N(x, y)$ can be generated using the interpolation approach, once the number of terms N in the series approximation has been specified. For both cases, $N = 25$ terms have been used in the series approximations. The matrix equations (51) and (52) for the series coefficients **a**

Table II. Boundary specifications, breakpoints and endpoint derivatives (if appropriate) for aquifer geometries

Top boundary		Bottom boundary	
Type	Breakpoints	Type	Breakpoints
	Aquifer 1		
Linear (5% slope)	[0,1] [50,3·5]	Linear (5% slope)	[0,0] [50,2·5]
	Aquifer 2		
Cubic spline	[0,0·348] [33,0·435] [67,0·696] [100,0·870]	Piecewise linear	[0,0] [33, −0·087] [67, −0·304] [100,0·304]
$f^t(0) = 0$	$f^t(100) = 0$		

and **b** proved to be well conditioned and were solved to machine precision using the IMSL linear systems subroutine library. Once the series coefficients have been calculated, the series expansion for the streamfunction $\psi_N(x, y)$ is also immediately obtained by involving the Cauchy–Riemann equations.

Using the series expansion for the hydraulic potential, a normalized potential Φ_N can be defined:

$$\Phi_N(x, y) = \frac{\phi_N(x, y) - \phi_{\min}}{\phi_{\max} - \phi_{\min}}, \tag{62}$$

where $\phi_{\max}$ and $\phi_{\min}$ are the maximum and minimum values of the potential function respectively. Similarly a normalized streamfunction $\Psi_N(x, y)$ can be defined:

$$\Psi_N(x, y) = \frac{\psi_N(x, y) - \psi_{\min}}{\psi_{\max} - \psi_{\min}}, \tag{63}$$

where $\psi_{\max}$ and $\psi_{\min}$ are the maximum and minimum values of the streamfunction respectively. Laplace's equation is known to satisfy a maximum principle,[22] hence the maximum and minimum values for the potential function and streamfunction can be determined by examining the flow boundaries.

The maximum value of the potential will occur at $[s, \eta(s)]$, while the minimum value of the streamfunction will occur at $[0, f^t(0)]$ (or anywhere on the impermeable boundary). The minimum value of the potential (and the maximum value of the streamfunction) can be determined numerically by dividing the boundary segments into a grid and comparing values at the grid points. The streamfunction will achieve a maximum on the soil surface and the flow will stagnate at this point.

The lines of equal hydraulic potential (or equipotentials) can be calculated by solving the implicit equation

$$\Phi_N(x, y) = p, \quad 0 \leqslant p \leqslant 1, \tag{64}$$

for y (or x). Similarly, streamlines can be calculated by solving numerically the implicit equation

$$\Psi_N(x, y) = p, \quad 0 \leqslant p \leqslant 1. \tag{65}$$

Figures 2 and 3 show steady flow solutions for aquifers 1 and 2 with equipotentials and streamlines corresponding to 10%, 30%, 50%, 70% and 90% of the potential and streamfunction ranges.

The equipotentials and streamlines form an orthogonal curvilinear set of co-ordinates. This is not immediately apparent owing to the large distortion of scale necessary to adequately display the solutions for both flow domains. The large aspect (i.e. length-to-depth) ratios of these aquifers are typical of the soil profiles encountered in hillside seepage problems. They also provide a good test for the interpolation method, as purely numerical schemes (such as the boundary integral method) can have difficulty in accurately resolving the fine detail in the flow domain. Fortunately the accuracy of the solution obtained using the interpolation approach can be rigorously quantified. In the next subsection the errors in the truncated series solution for each aquifer are provided.

5.2. Iterative scheme and boundary errors

At the start of the iterative process the water table is approximated by one spline segment, until the estimated recharge at the breakpoints (59) satisfies the error tolerance

$$\left|\frac{\hat{R}_j - R}{R}\right| \leqslant 10^{-3}. \tag{66}$$

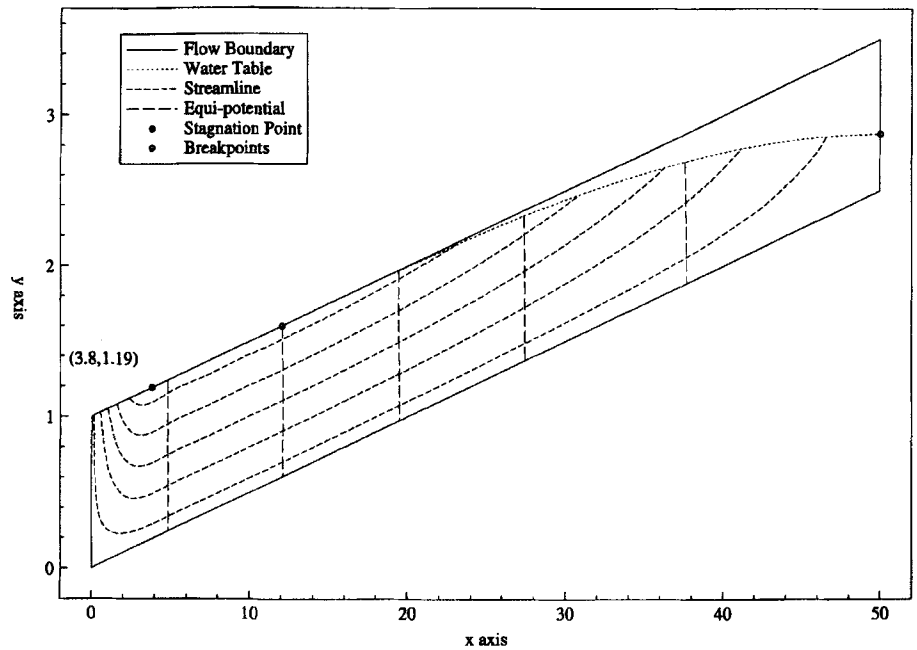

Figure 2. Steady water table, equipotentials and streamlines for aquifer 1

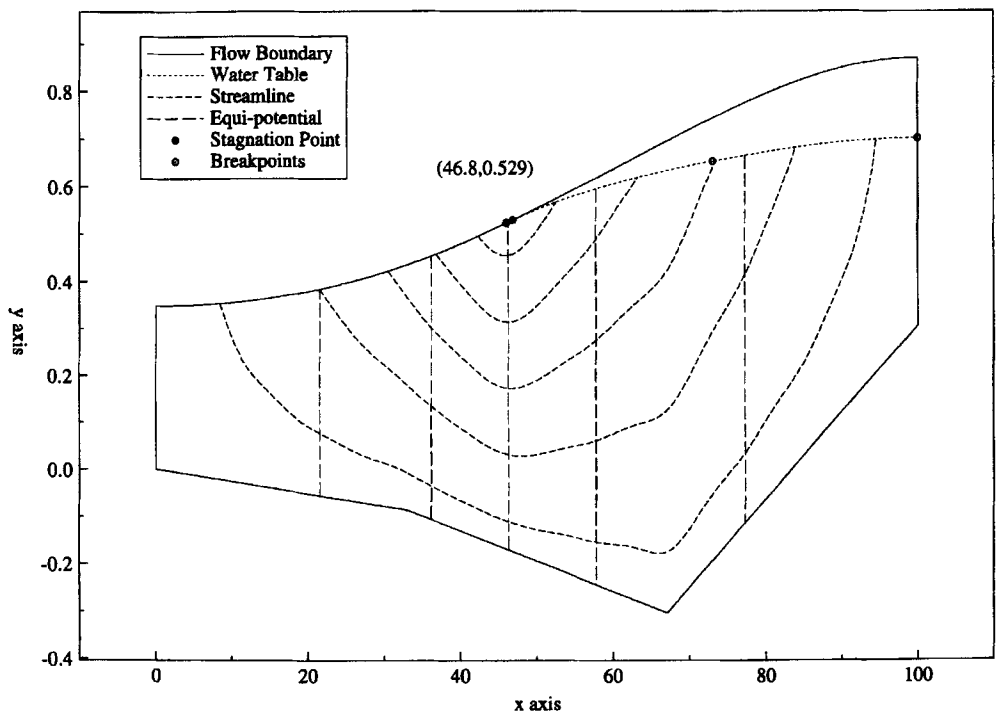

Figure 3. Steady water table, equipotentials and streamlines for aquifer 2

Once this error condition has been met, additional spline segments can be added and the iterative process continued until (once again) the error tolerance is satisfied. Spline segments can be added in this fashion until the required accuracy in the free boundary condition is obtained. For aquifer 1, one spline segment was sufficient, while two segments were needed for aquifer 2.

The error in the solution can be divided into two parts, namely the truncation error in the series approximation and the free boundary error. The truncation error $\varepsilon_N(x, y)$ at any point in the solution domain is defined by

$$\varepsilon_N(x, y) = \phi(x, y) - \phi_N(x, y), \tag{67}$$

where $\phi(x, y)$ is the exact solution and $\phi_N(x, y)$ is the truncated series approximation. Applying the Laplacian operator to (67) and noting that the truncated series satisfies Laplace's equation exactly, then

$$\nabla^2 \varepsilon_N(x, y) = \nabla^2 \phi(x, y) - \nabla^2 \phi_N(x, y) = 0. \tag{68}$$

Hence $\varepsilon_N(x, y)$ satisfies Laplace's equation, the governing differential equation. As noted above, Laplace's equation obeys a maximum principle and so the maximum error in the series approximation can be determined by examining the boundary errors.

The root mean square (RMS) error $\varepsilon_N^{\mathrm{b}}$ in the bottom boundary approximation (3) can be obtained directly from the residual errors along the bottom flow boundary (31) as

$$\varepsilon_N^{\mathrm{b}} = \left(\frac{1}{s} \int_0^s \left[R_N^{\mathrm{b}}(x; \mathbf{a}, \mathbf{b}) \right]^2 \mathrm{d}x \right)^{1/2}. \tag{69}$$

Similarly the RMS error $\varepsilon_N^{\mathrm{t}}$ in the top boundary approximation (5) can be obtained from (32) as

$$\varepsilon_N^{\mathrm{t}} = \left(\frac{1}{s} \int_0^s \left[R_N^{\mathrm{t}}(x; \mathbf{a}, \mathbf{b}) \right]^2 \mathrm{d}x \right)^{1/2}. \tag{70}$$

Table III lists the top and bottom boundary RMS errors for both flow solutions obtained above by the interpolation method with $N = 25$.

The free boundary error is reduced during the iterative process until it is approximately the same magnitude as the top boundary error. The RMS error ε_N^{ψ} in the streamfunction cost function (55) is given by

$$\varepsilon_N^{\psi} = \left(\frac{1}{r} \int_r^s \left\{ \psi[x, \eta(x)] - R(s - x) \right\}^2 \mathrm{d}x \right)^{1/2} \tag{71}$$

and its values for aquifers 1 and 2 are included in Table III. For aquifer 1, roughly 40 iterations were necessary to obtain sufficient accuracy for the streamfunction condition, while almost 90 iterations were necessary for aquifer 2. In the second case the streamfunction error could not be reduced enough with one spline segment, so two spline segments were used after approximately 40 iterations.

The accuracy of the truncated series approximation will obviously depend on N, the number of terms in the series. The eigenfunction expansion method minimizes the average squared error in the boundary approximations, whereas the interpolation method forces the residual errors to be zero at a discrete set of

Table III. Root mean square errors in top and bottom boundary conditions and RMS error in (free boundary) streamfunction condition

	$\varepsilon_N^{\mathrm{b}}$	$\varepsilon_N^{\mathrm{t}}$	ε_N^{ψ}
Aquifer 1	$3{\cdot}6 \times 10^{-4}$	$4{\cdot}6 \times 10^{-3}$	$7{\cdot}3 \times 10^{-4}$
Aquifer 2	$1{\cdot}1 \times 10^{-5}$	$2{\cdot}8 \times 10^{-5}$	$4{\cdot}3 \times 10^{-5}$

points. For the solutions presented here, more terms were necessary in the series approximation when the series coefficients were estimated using the interpolation method, to satisfy the same error tolerances. Some experimentation revealed that roughly twice the number of terms were needed for the interpolation method to produce comparable boundary errors to the eigenfunction expansion method. However, an examination of Table I reveals that the computational cost of doubling the number of terms for the interpolation method is insignificant compared with the cost of the eigenfunction expansion estimators.

6. DISCUSSION

In the preceding sections an interpolation approach has been used to provide an analytic series solution for Laplace's equation with irregular boundary geometry, in the context of a free boundary problem. The interpolation approach is simple to understand and implement, as well as providing a very efficient solution process. This is particularly evident as the number of terms, N, in the series increases.

The eigenfunction expansion method provides a theoretical framework for the validity of the interpolation method and can also be used to generate the series coefficients. However, the cost of generating each matrix entry is proportional to N, whereas the matrix entries in the interpolation method are generated in roughly constant time. Although more terms in the series approximation appear necessary using the interpolation method, the overall efficiency of the method completely offsets this slight disadvantage.

Owing to the choice of basis functions in the analytic series, the solutions produced encompass all the advantages of an analytic solution for the potential problem. One of these advantages is the immediate availability of the streamfunction, so that both the potential and streamfunction representations can be used simultaneously if required. As a consequence, equipotentials and streamlines can be efficiently and accurately calculated once the series coefficients have been estimated. Another significant feature is that exact error estimates are immediately obtainable by examining the boundary errors. The interpolation approach to the series coefficient estimation has been shown here to produce a robust and highly efficient vehicle for the solutions of a wide range of potential flow problems.

REFERENCES

1. O. D. Kellogg, *Foundations of Potential Theory*, Dover, New York, 1953.
2. J. A. Liggett and P. L. -F. Liu, *The Boundary Integral Equation Method for Porous Media Flow*, Allen and Unwin, London, 1983.
3. E. O. Frind and G. G. Matanga, 'The dual formation of flow for contaminant transport modeling, I: Review of theory and accuracy aspects', *Water Resources Res.*, **21**, 159–169 (1985).
4. C. Canuto, M. -Y. Hussaini, A. Quarteroni and T. A. Zang, *Spectral Methods in Fluid Dynamics*, Springer, New York, 1988.
5. J. P. Boyd, in C. A. Brebbia and S. A. Orszag (eds), *Chebyshev and Fourier Spectral Methods*, Springer, New York, 1989.
6. G. F. Carrier, M. Krook and C. E. Pearson, *Functions of a Complex Variable*, McGraw-Hill, New York, 1966.
7. G. F. Carrier and C. E. Pearson, in R. E. O'Malley Jr. (ed.), *Ordinary Differential Equations*, Society for Industrial and Applied Mathematics, Philadelphia, PA, 1991.
8. W. W. Read and R. E. Volker, 'Series solutions for steady seepage through hillsides with arbitrary flow boundaries', *Water Resources Res.*, **29**, 2871–2880 (1993).
9. W. W. Read and R. E. Volker, 'BIEM/QLS computer generated solutions for sloping base seepage problems', *Comput. Fluids*, **23**, 115–124 (1994).
10. W. W. Read and R. E. Voker, 'A computationally efficient solution technique to Laplacian flow problems with mixed boundary conditions', in *Computational Techniques and Applications: CTAC '89*, Hemisphere, Washington, DC, 1990, pp. 707–714.
11. W. W. Read, 'Series solutions for Laplace's equation with non-homogeneous mixed boundary conditions and irregular boundaries', *Math. Comput. Model.*, **17**(12), 9–19 (1993); 'Errata', *Math. Comput. Models*, **18**(7), 107 (1993).
12. W. W. Read, 'A comparison of analytical series methods for Laplacian free boundary problems', *Math. Comput. Model.*, **20**(12), 31–44 (1994).
13. P. J. Davis, *Interpolation and Approximation*, Blaisdell, Waltham, MA, 1963.
14. S. D. Conte and C. De Boor, *Elementary Numerical Analysis: An Algorithmic Approach*, McGraw-Hill, New York, 1980.

15. W. E. Boyce and R. C. DiPrima, *Elementary Differential Equations and Boundary Value Problems*, Wiley, New York, 1986.
16. F. M. Arscott and A. Darai, 'Curvilinear co-ordinate systems in which the Helmholtz equation separates', *IMA J. Appl. Math.*, **27**, 33–70 (1981).
17. W. L. Powers, D. Kirkham and G. Snowden, 'Orthonormal function tables and the seepage of steady rain through soil bedding', *J. Geophys. Res.*, **72**, 6225–6237 (1967).
18. M. S. Selim and D. Kirkham, 'Seepage through soil bedding or a hillside due to a steady rainfall: II. Soil surface of arbitrary shape', *Soil Sci. Soc. Am. Proc.*, **36**, 407–412 (1972).
19. N. L. Powell and D. Kirkham, 'Flow patterns of steady rainfall seeping through bedded land or a hillside with a barrier at great depth', *J. Hydrol.*, **23**, 203–217 (1974).
20. W. W. Read and R. E. Volker, 'Prediction of water table location for irrigated hillslopes', *Res. Bull.*, Department of Civil and Systems Engineering, James Cook University of North Queensland, Townsville, 1987.
21. B. A. Finlayson, *The Method of Mean Weighted Residuals and Variational Principles*, Academic, New York, 1972.
22. D. Gilbarg and N. S. Trudinger, *Elliptic Partial Differential Equations of Second Order*, 2nd edn, Springer, Berlin, 1983.